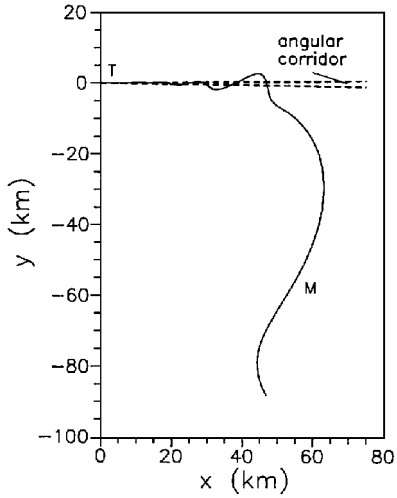

Fig. 4 Rendezvous trajectory: ODRRCA-based scheme.

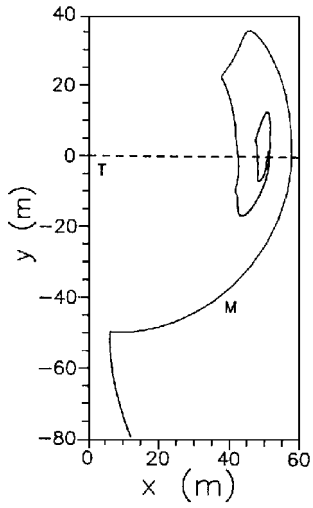

Fig. 5 Round flight trajectory: combined scheme.

also small. A cost to pay is the relatively complex two-component propulsion system needed.

Combined Scheme

This scheme is a combination of the two preceding ones. The entire rendezvous operation is divided into two steps. In the first step, which is called the main part and starts at the beginning of the terminal rendezvous, the RRCA-based scheme is applied until the maneuvering spacecraft arrives at a designed end distance (for example, 50 m) from the target spacecraft. At this moment the second step, called the round flight, begins. In this step, the ODRRCA-based scheme takes the place of the RRCA-based scheme. By properly setting the sign and magnitude of k near zero, the distance between the two spacecraft does not change significantly. Rather, the maneuvering spacecraft flies by the target spacecraft and finally stops at a desirable position, determined by the parameter φ_d. The value of φ_d is assigned by the mission designer. The trajectory in the main part of the combined scheme is the same as shown in Fig. 3, and Fig. 5 shows the round flight part of the trajectory. The combined scheme preserves the advantages of the two previous schemes with fewer complications of the propulsion system.

Conclusions

The RRCA and the ODRRCA are nonlinear control algorithms. They are, in particular, suitable for the control of the relative motion between two spacecraft such as the tethered satellite maneuver, space rendezvous, etc. Based on these algorithms, three generalized control schemes for terminal rendezvous have been proposed: the RRCA-based scheme, the ODRRCA-based scheme, and the combined scheme. Various rendezvous missions in both circular and elliptic orbits can be carried out by these schemes with variable-thrust or fixed-thrust engines. For a typical terminal rendezvous started at a separation distance of 100 km, the fuel consumption of the maneuvering spacecraft with initial mass of 7800 kg is about 175 kg, and the time required to complete the rendezvous is about 220 min. The distance between two spacecraft as well as the distance rate decrease in an exponential manner, while the rendezvous trajectory can be placed in a desirable position to meet the mission requirements.

Acknowledgment

The author is grateful to Robert G. Melton of Pennsylvania State University for his valuable comments on this and other papers of the author.

References

[1] Clohessy, W. H., and Wiltshire, R. S., "Terminal Guidance System for Satellite Rendezvous," *Journal of the Aerospace Sciences*, Vol. 27, 1960, pp. 653–658.

[2] Balakhontsev, V. G., Ivanov, V. A., and Shabanov, V. I., *Rendezvous in Space*, M:Voinizdat, Ministry of Defence, Moscow, 1973, Chap. 5.

[3] Yu, S.-H., "Terminal Spacecraft Coplanar Rendezvous Control," *Journal of Guidance, Control, and Dynamics*, Vol. 18, No. 4, 1995, pp. 838–842.

[4] Yu, S.-H., "Control of Omni-Directional Rendezvous Trajectories," *Acta Astronautica*, Vol. 12, No. 2, 1994, pp. 83–87.

[5] Guliaev, V. I., Bazhenov, V. A., and Gotsuliak, E. A., *Stability of Periodic Processes in Nonlinear Mechanical Systems*, Lvov Univ., Lvov, Ukraine, 1983, Chap. 1.

[6] Yu, S., "Periodic Motion in the Tethered Satellite System," *Journal of Guidance, Control, and Dynamics*, Vol. 19, No. 5, 1996, pp. 1195–1197.

Optimized TRIAD Algorithm for Attitude Determination

Itzhack Y. Bar-Itzhack* and Richard R. Harman†
NASA Goddard Space Flight Center, Greenbelt, Maryland 20771

I. Introduction

WHEN the components of two abstract vectors are given in two different coordinate systems, it is possible to find the orientation difference between the two systems. In particular, we can easily find the transformation matrix from one coordinate system to the other. TRIAD[1,2] is an algorithm that does just that. The process of finding the matrix using TRIAD is as follows. Let $\boldsymbol{w}_1$ and $\boldsymbol{w}_2$ denote the column matrices whose elements are, respectively, the components of the two abstract vectors when resolved in one coordinate system (typically a body frame), and let $\boldsymbol{v}_1$ and $\boldsymbol{v}_2$ denote the column matrices whose elements are, respectively, the components of the abstract vectors when resolved in the other coordinate system (typically a reference frame). The algorithm calls for the computation of the following column matrices in the body frame:

$$\boldsymbol{r}_1 = \boldsymbol{w}_1/|\boldsymbol{w}_1| \tag{1a}$$

$$\boldsymbol{r}_2 = \frac{(\boldsymbol{r}_1 \times \boldsymbol{w}_2)}{|\boldsymbol{r}_1 \times \boldsymbol{w}_2|} \tag{1b}$$

$$\boldsymbol{r}_3 = \boldsymbol{r}_1 \times \boldsymbol{r}_2 \tag{1c}$$

Received April 11, 1996; revision received July 15, 1996; presented as Paper 96-3616 at the AIAA/AAS Astrodynamics Specialist Conference, San Diego, CA, July 29–31, 1996; accepted for publication Aug. 21, 1996.

*Senior Research Associate, Flight Mechanics Branch, Code 552; currently Sophie and William Shamban Professor of Aerospace Engineering, Faculty of Aerospace Engineering, and Member, Technion Space Research Institute, Technion—Israel Institute of Technology, Haifa 32000, Israel. Associate Fellow AIAA.

†Aerospace Engineer, Flight Mechanics Branch, Code 552.

and the following corresponding column matrices in the reference frame:

$$s_1 = v_1/|v_1| \tag{2a}$$

$$s_2 = \frac{(s_1 \times v_2)}{|s_1 \times v_2|} \tag{2b}$$

$$s_3 = s_1 \times s_2 \tag{2c}$$

Then the attitude matrix A that transforms a vector from the body frame to the reference frame is computed as follows:

$$A = r_1 \cdot s_1^T + r_2 \cdot s_2^T + r_3 \cdot s_3^T \tag{3}$$

where T denotes the transpose.

Following the process indicated in Eqs. (1) and (2), we realize that the vector that is designated first is normalized, but otherwise remains intact, whereas the other vector serves as a means to define the second vector in the triad pair, which determines the attitude. There is, therefore, a biased consideration of the two vectors where the first is given a preference in the determination of A. We say that the first vector serves as an anchor in the computation of the transformation matrix. It is, indeed, a good engineering practice to use the vector measured by the most accurate device as the anchor vector. For example, it is very logical to use the vector measured by a star tracker as the anchor when the other vector is measured by magnetometers. However, we show in this Note that the TRIAD solution is not optimal, and we develop a new algorithm, called the Optimized TRIAD, which provides an improved solution.

II. Optimized TRIAD

The accuracy of each vector-measuring device is quantified by the standard deviation of its error. The vector measured by a star tracker is assigned a standard deviation smaller than that assigned to a magnetometer, for example. Borrowing this notion, we assign a standard deviation to the TRIAD-computed attitude matrix that corresponds to the standard deviation of the anchor vector used in computing the matrix. Therefore, the attitude matrix A_1, in whose computation vector number 1 is used as the anchor, is assigned the standard deviation σ_1, which is the standard deviation of vector number 1. Similarly, if vector number 2 serves as the anchor, we denote the computed attitude matrix by A_2 and assign to it the standard deviation σ_2, which is the standard deviation of vector number 2. Actually, because the computation that yields the matrix is nonlinear and is based on both vectors, there is no simple linear relation between the standard deviation of the anchor vector and that of the resulting matrix, but because we are concerned only with the relative accuracies of A_1 and A_2, the expression of their accuracy by σ_1 and σ_2, respectively, well fits our final purpose.

It is well known that when y_1 and y_2 are independent unbiased scalar measurements of an unknown scalar x and their measurement errors have standard deviations σ_1 and σ_2, respectively, then $\hat{x}$, the linear unbiased minimum variance estimate of x, is given by[3]

$$\hat{x} = \frac{\sigma_2^2}{\sigma_1^2 + \sigma_2^2} y_1 + \frac{\sigma_1^2}{\sigma_1^2 + \sigma_2^2} y_2 \tag{4}$$

The use of this algorithm implies that we know both σ_1 and σ_2. We have to ask ourselves how good the estimate is when this is not the case. To answer this question, let us assume that we use the wrong standard deviation s_1 instead of the correct value σ_1 and, similarly, we use s_2 instead of σ_2. Then instead of the estimate given by Eq. (4), we obtain

$$\hat{x} = \frac{s_2^2}{s_1^2 + s_2^2} y_1 + \frac{s_1^2}{s_1^2 + s_2^2} y_2 \tag{5}$$

Defining $k_1 = s_2^2/(s_1^2 + s_2^2)$, Eq. (5) can be written as

$$\hat{x} = k_1 y_1 + (1 - k_1) y_2 \tag{6}$$

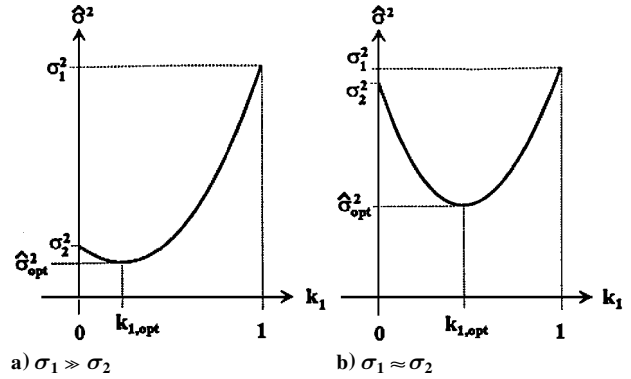

Fig. 1 Relationship between the variance of the estimate and k_1.

Defining the estimation error e as $\hat{x} - x$, it is easy to show that $\hat{\sigma}^2$, the variance of $\hat{x}$, is

$$\hat{\sigma}^2 = k_1^2 \sigma_1^2 + (1 - k_1)^2 \sigma_2^2 \tag{7}$$

or

$$\hat{\sigma}^2 = \left(\sigma_1^2 + \sigma_2^2\right) k_1^2 - 2\sigma_2^2 k_1 + \sigma_2^2 \tag{8}$$

Obviously, the minimum (optimal) $\hat{\sigma}^2$ is achieved when

$$k_1 = k_{1,\text{opt}} = \frac{\sigma_2^2}{\sigma_1^2 + \sigma_2^2} \tag{9}$$

Then by substitution of Eq. (9) into Eq. (8), we have

$$\hat{\sigma}^2 = \hat{\sigma}^2_{\text{opt}} = \frac{\sigma_1^2 \sigma_2^2}{\sigma_1^2 + \sigma_2^2} \tag{10}$$

From the definition of k_1 it is clear that $0 \le k_1 \le 1$ whether or not s_1 and s_2 are the correct respective values of σ_1 and σ_2. From Eq. (8) it is also clear that the curve that describes the functional relation between $\hat{\sigma}^2$ and k_1 is a parabola. Two cases of this parabola are presented in Figs. 1a and 1b. In Fig. 1a there is a big difference between the accuracy of the measuring devices. Therefore, σ_1^2 (which, with no loss of generality, we assume to be the larger of the two) is much bigger than σ_2^2. In Fig. 1b, σ_1^2 is close to σ_2^2. From the definition of k_1 and the two cases presented in Fig. 1, one can easily arrive at the following conclusions.

1) When one uses the correct standard deviations in Eq. (5), $k_1 = k_{1,\text{opt}}$ and $\hat{\sigma} = \hat{\sigma}_{\text{opt}}$.

2) Because $0 \le k_1 \le 1$, then $\hat{\sigma} \le \sigma_1$ (assuming, as before, that σ_1 is the larger standard deviation).

3) The gain k_1 depends on the ratio s_1/s_2 and not on s_1 and s_2 themselves.

4) When $\sigma_1 \approx \sigma_2$, then for almost any ratio s_1/s_2 one obtains $\hat{\sigma} \le \sigma_2$ (see Fig. 1b); that is, in this case, the sensitivity of the estimator to a wrong ratio is small.

5) If the ratio s_1/s_2 is not far from the ratio σ_1/σ_2, then even when $\sigma_2 \ll \sigma_1$ (see Fig. 1a), almost always $\hat{\sigma} \le \sigma_2$ and certainly $\hat{\sigma} \le \sigma_1$.

We conclude from the preceding analysis that the algorithm of Eq. (4) is fairly robust to errors in the measurement statistics.

Following Eq. (4), we postulate that given A_1, with its assigned standard deviation σ_1, and A_2, with its assigned standard deviation σ_2, we can find $\hat{A}'$, an estimate of A that is better than either A_1 or A_2, when using the estimator of Eq. (4); that is,

$$\hat{A}' = \frac{\sigma_2^2}{\sigma_1^2 + \sigma_2^2} A_1 + \frac{\sigma_1^2}{\sigma_1^2 + \sigma_2^2} A_2 \tag{11}$$

An interesting aspect of this estimator [as well as that of Eq. (4)] is the conclusion that proper blending of the worse result with the better may yield an estimate whose accuracy is greater than that of the

better (see Fig. 1). Because $\hat{A}'$ is a result of the addition of functions of two orthogonal matrices, it is not necessarily orthogonal, and thus is not a legitimate attitude matrix unless it is orthogonalized. However, because $\hat{A}'$ is close to being orthogonal, one orthogonalization cycle, as described in Ref. 4, suffices:

$$\hat{A} = 0.5[\hat{A}' + (\hat{A}'^{-1})^T] \tag{12}$$

Note that the inversion of $\hat{A}'$ is an easy task since the inverse of a 3×3 matrix can be computed analytically. It is cumbersome, if not impossible, to prove analytically that $\hat{A}$ is better than either A_1 or A_2; however, we can try to show it empirically, as demonstrated in the next section.

III. Algorithm Testing

A. Static Testing

In the static testing, we chose some fixed attitude matrix, A_{true}, and the components of the unit vectors $\boldsymbol{v}_1$ and $\boldsymbol{v}_2$ (two abstract vectors resolved in the reference system). Then A_{true} was used to transform $\boldsymbol{v}_1$ and $\boldsymbol{v}_2$ to the body system. To each component of the latter we added white measurement noise drawn from a random number generator. The added noise was unbiased and had a standard deviation $\sigma_1 = 0.2$ for the noise added to the components of the transformed $\boldsymbol{v}_1$ and $\sigma_2 = 0.1$ for the noise added to the components of the transformed $\boldsymbol{v}_2$. The noisy column matrices were designated as $\boldsymbol{w}_1$ and $\boldsymbol{w}_2$. TRIAD was then applied to the four column matrices as described in the preceding section, once when vector number 1 was used as the anchor and once when the other was used as the anchor. This generated the attitude matrices A_1 and A_2 respectively, which then were used in Eqs. (11) and (12) to generate $\hat{A}'$ and the optimized orthogonal matrix $\hat{A}$. The quaternions corresponding to A_{true}, A_1, A_2, and $\hat{A}$ were computed and denoted by $\boldsymbol{q}_{\text{true}}$, $\boldsymbol{q}_1$, $\boldsymbol{q}_2$, and $\hat{\boldsymbol{q}}$, respectively. The error quaternion of each transformation was computed as follows:

$$\delta\boldsymbol{q} = \boldsymbol{q}^{-1} \otimes \boldsymbol{q}_{\text{true}} \tag{13}$$

where $\otimes$ denotes quaternion multiplication. Therefore, when $\boldsymbol{q}$ corresponded to $\boldsymbol{q}_1$ we obtained $\delta\boldsymbol{q}_1$, when $\boldsymbol{q}$ corresponded to $\boldsymbol{q}_2$ we obtained $\delta\boldsymbol{q}_2$, and when $\boldsymbol{q}$ corresponded to $\hat{\boldsymbol{q}}$ we obtained $\delta\hat{\boldsymbol{q}}$. [Note that with the choice of Eq. (13) for computing the erroneous quaternion, we assume that $\delta\boldsymbol{q}$ is the transformation quaternion from the erroneous to the true coordinate system.] Finally, we extracted from each $\delta\boldsymbol{q}$ the corresponding rotation angle $\delta\varphi$. We thus have expressed the error in the computation of the attitude by a single angular error. That error was the angle by which the computed coordinate system had to be rotated about the appropriate Euler axis to coincide with the true body coordinates.

Since $\delta\varphi$ is a random variable, we ran 100 runs (realizations), each for 60 s and each starting with a different seed. Along the time axis the computation was performed every second. We then averaged the 100 realizations at each time point and obtained the ensemble average of each error; that is, we obtained

$$\delta\bar{\varphi}_1(t_k) = \frac{1}{100}\sum_{j=1}^{100}\delta\varphi_{1,j}(t_k) \tag{14a}$$

$$\delta\bar{\varphi}_2(t_k) = \frac{1}{100}\sum_{j=1}^{100}\delta\varphi_{2,j}(t_k) \tag{14b}$$

$$\delta\bar{\hat{\varphi}}(t_k) = \frac{1}{100}\sum_{j=1}^{100}\delta\hat{\varphi}_j(t_k) \tag{14c}$$

where j denotes the number of the realization and t_k denotes the point in time where TRIAD and Optimized TRIAD were performed. The values of $\delta\bar{\varphi}_1(t_k)$, $\delta\bar{\varphi}_2(t_k)$, and $\delta\bar{\hat{\varphi}}(t_k)$ as function of t_k are presented in Fig. 2, where we observe that $\delta\bar{\hat{\varphi}}$ is consistently smaller than the other two functions. We also computed the running time

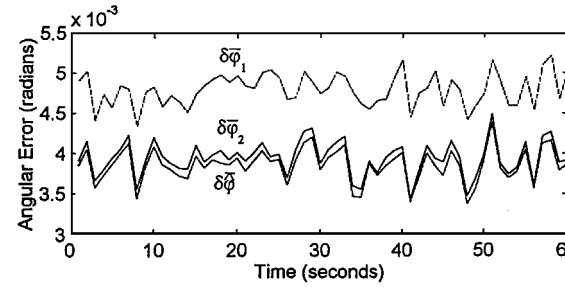

Fig. 2 Ensemble average of the error associated with A_1, A_2, and $\hat{A}$.

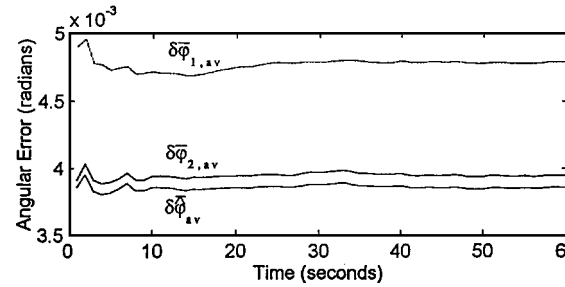

Fig. 3 Running time average of the ensemble average of the error associated with A_1, A_2, and $\hat{A}$.

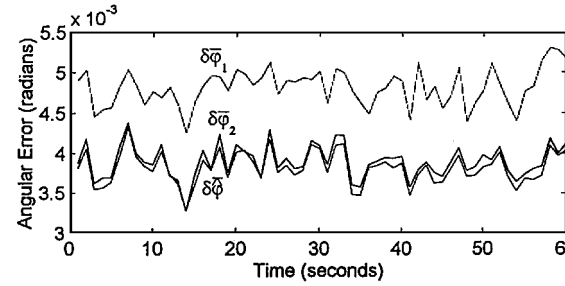

Fig. 4 Ensemble average of the error associated with A_1, A_2, and $\hat{A}$ for a time-varying A_{true}.

average of each ensemble average from the beginning of the run to time t_k. In other words, we computed

$$\delta\bar{\varphi}_{1,\text{av}}(t_k) = \frac{1}{k}\sum_{i=1}^{k}\delta\bar{\varphi}_1(t_i) \tag{15a}$$

$$\delta\bar{\varphi}_{2,\text{av}}(t_k) = \frac{1}{k}\sum_{i=1}^{k}\delta\bar{\varphi}_2(t_i) \tag{15b}$$

$$\delta\bar{\hat{\varphi}}_{\text{av}}(t_k) = \frac{1}{k}\sum_{i=1}^{k}\delta\bar{\hat{\varphi}}(t_i) \tag{15c}$$

The value of $\delta\bar{\varphi}_{1,\text{av}}(t_k)$, $\delta\bar{\varphi}_{2,\text{av}}(t_k)$, and $\delta\bar{\hat{\varphi}}_{\text{av}}(t_k)$ as function of t_k are presented in Fig. 3, where it is once again observed that $\hat{A}$ is superior to both A_1 and A_2. In other words, on the average, the Optimized TRIAD yields better results for the case tested.

B. Dynamic Testing

To examine the influence of changing attitude, we repeated the same runs and computations as described before, with the body rotating at 1 rpm about an axis $\bar{\rho}$ defined as follows:

$$\bar{\rho} = \frac{1}{\sqrt{3}}[\bar{i}_b, \bar{j}_b, \bar{k}_b] \tag{16}$$

The results of this case, similar to those for the static test, are presented in Figs. 4 and 5. It is clear that the Optimized TRIAD algorithm outperforms the TRIAD algorithm for this test even when the most accurately measured vector serves as the anchor in the application of TRIAD.

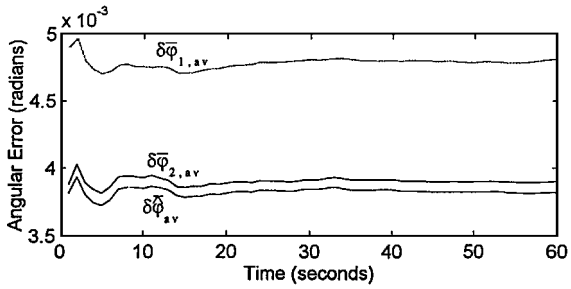

Fig. 5 Running time average of the ensemble average of the error associated with A_1, A_2, and $\hat{A}$ for a time-varying A_{true}.

Because the idea behind this algorithm is borrowed from linear estimation theory of independent unbiased measurement errors, one would expect the ensemble average of the angular error to be zero; however, as can be seen in Figs. 2 and 4, this is not the case. This discrepancy stems from the fact that the displayed error is not linearly related to the averaged matrices. Also, the errors in the computed matrices A_1 and A_2 are not really independent.

Finally, the vectors v_1 and v_2, which are the components of the two abstract vectors resolved in the reference coordinates, were constant through all runs, and the angle between the two vectors was close to 90 deg. To investigate the behavior of the algorithm for a different separation angle, we chose two new v_1 and v_2 vectors with a separation angle close to 45 deg and performed the dynamic test case. The results were similar to those presented in Figs. 4 and 5; however, the errors of all three algorithms were nearly 25% higher, as expected.

IV. Conclusions

We have presented a simple TRIAD-based algorithm, which we call Optimized TRIAD, that consistently outperformed TRIAD in simulated studies. The algorithm consists of solving TRIAD twice, once with one vector as the anchor and once with the other vector as the anchor, weight averaging the two resultant matrices, and orthogonalizing the final matrix. The weights are determined by the statistics of the measuring devices that produced the vector measurements. The idea behind this algorithm is borrowed from linear estimation theory of independent unbiased measurement errors. However, although the blending of the two TRIAD-generated matrices is based on an unbiased minimum variance formula, the ensemble average of the angular error is not zero because the error is not linearly related to the averaged matrices. Also, the errors in the computed matrices A_1 and A_2 are not really independent.

We have shown empirically that, indeed, the accuracy of the Optimized TRIAD is better than that of TRIAD even when the latter uses the vector measured most accurately as the anchor. Note though that in this statement we refer to the average performance; that is, occasionally TRIAD may yield results that are better than those obtained using Optimized TRIAD, but on the average, Optimized TRIAD performs better. Similar to a Kalman filter, the proper blending of the better with the worse TRIAD-generated attitude matrices yields, on the average, a result that is more accurate than the better of the two TRIAD solutions.

Acknowledgment

This work was performed while Itzhack Y. Bar-Itzhack was on a National Research Council–NASA Goddard Space Flight Center Research Associateship.

References

[1]Black, H. D., "A Passive System for Determining the Attitude of a Satellite," *AIAA Journal*, Vol. 2, No. 7, 1964, pp. 1350, 1351.

[2]Shuster, M. D., and Oh, S. D., "Three-Axis Attitude Determination from Vector Observations," *Journal of Guidance and Control*, Vol. 4, No. 1, 1981, pp. 70–77.

[3]Gelb, A. (ed.), *Applied Optimal Estimation*, MIT Press, Cambridge, MA, 1988, pp. 5, 6.

[4]Bar-Itzhack, I. Y., and Meyer, J., "On the Convergence of Iterative Orthogonalization Processes," *IEEE Transactions on Aerospace and Electronic Systems*, Vol. AES-12, No. 2, 1976, pp. 146–151.

Characterization of Ring Laser Gyro Performance Using the Allan Variance Method

Lawrence C. Ng*
Lawrence Livermore National Laboratory, Livermore, California 94511
and
Darryll J. Pines†
University of Maryland, College Park, Maryland 20742-3015

Introduction

THE ring laser gyro (RLG) has become a common instrument in strapdown inertial navigation systems for spacecraft and other aerospace systems. Current RLGs can sense angular rates as low as 0.001 deg/h. The RLG's ability to measure angular rate has several limitations including lock-in, stability, linearity and alignment errors. These limitations contribute to the static noise statistics of the gyro. Static characterization of RLG performance has received much attention since its inception.[1] Performance tests on the RLG have revealed many error sources, such as 1) angle random walk, 2) quantization, 3) bias instability, 4) rate angle walk, 5) rate ramp, 6) sinusoidal component, and 7) scale factor nonlinearity. The first three error terms are normally included as part of the overall performance specifications of an RLG given by the manufacturer. However, traditional approaches such as computing the sampled mean and variance from a measurement set do not reveal the latter five error sources. Although computations of the autocorrelation function or the power spectral density (PSD) distribution do contain a complete description of the error sources, these results are difficult to interpret or extract.

This Engineering Note describes the Allan variance method and its application to the characterization of an RLG's performance[2] under quasisteady state conditions. The method was initially developed by David Allan of the National Bureau of Standards to quantify the error statistics of a cesium beam frequency standard employed by the U.S. Frequency Standards in the 1960s.[3] In general, the method can be applied to analyze the error characteristics of any precision measurement instrument. The key attribute of the method is that it allows for a finer, easier characterization and identification of error sources and their contribution to the overall noise statistics. This Engineering Note presents an overview of the cluster analysis method,[4] explains the relationship between Allan variance and PSD distribution of underlying noise sources, and describes the batch and recursive implementation approaches.

Method of Cluster Analysis

Let angular rate data ω be taken at a rate of f_s samples per second; then from a collection of N data points, we form $K = N/M$ clusters, where M is the number of samples per cluster. The second step is to compute the average for each cluster from the expression

$$\varpi_k(M) = \frac{1}{M}\sum_{i=1}^{M} \omega_{(k-1)M+i}, \qquad k = 1, \ldots, K \tag{1}$$

Received July 26, 1996; revision received Sept. 17, 1996; accepted for publication Sept. 18, 1996. This paper is declared a work of the U.S. Government and is not subject to copyright protection in the United States.

*Member, Technical Staff, Electrical Engineering Division.

†Assistant Professor, Department of Aerospace Engineering. Senior Member AIAA.